I&EC research
Industrial & Engineering Chemistry Research

Article

LaBO3 (B: Mn, Fe, Co, Ni, Cu and Zn) Catalysts for CO + NO Reaction

Behrang Izadkhah, Aligholi Niaei, María José Illan-Gomez, Dariush Salari, Ali Tarjomannejad, and Vicente Albaladejo-Fuentes

Ind. Eng. Chem. Res., **Just Accepted Manuscript** • DOI: 10.1021/acs.iecr.7b00457 • Publication Date (Web): 13 Mar 2017

ACS Publications

Industrial & Engineering Chemistry Research is published by the American Chemical Society. 1155 Sixteenth Street N.W., Washington, DC 20036

$LaBO_3$ (B: Mn, Fe, Co, Ni, Cu and Zn) Catalysts for CO + NO Reaction

Behrang Izadkhah[1,3], Aligholi Niaei*[3], María José Illán-Gómez[2], Dariush Salari[1], Ali Tarjomannejad[3], Vicente Albaladejo-Fuentes[2]

[1]Department of Applied Chemistry, Faculty of Chemistry, University of Tabriz, 5166616471 Tabriz, Iran

[2]Carbon Materials and Environment Research Group, Department of Inorganic Chemistry, Faculty of Science, University of Alicante, E-03080 Alicante, Spain

[3]Catalyst & Reactor Research Group, Department of Chemical & Petroleum Engineering, University of Tabriz 5166616471, Tabriz, Iran

[*] Email addresses: aniaei@tabrizu.ac.ir & niaei@yahoo.com, Tel: +984113393158, Fax: +984113340191

Abstract

A series of transition metals $LaBO_3$ perovskites (B= Mn, Fe, Co, Ni, Cu and Zn) has been synthesized and tested as catalysts for simultaneous removal of CO and NO in a fixed bed reactor. To improve the catalytic activity of $LaFeO_3$, as the most active formulation, it has been modified by using other active metals (Mn, Co and Cu) for partial substitution of Fe in the perovskite formulation ($LaFe_{0.7}M_{0.3}O_3$). The results revealed that Mn substitution improves significantly the catalytic activity because increases the Mn (IV) to Mn (III) ratio leading to the generation of a large amount of structural defects and, also, because increases the amount of reducible active sites.

Keywords. Perovskite, NOx reduction, NO+CO reaction, Catalytic reduction, Air pollution.

Introduction

The removal of CO and NO has attracted a great attention because of their presence in mobile and static exhaust sources. Photochemical smog and acid rain formation are the main problems caused by NOx emissions. For the removal of NOx, different strategies including selective catalytic reduction (SCR) using CO, NH_3 and thermal degradation have been used. Because of the toxic nature of CO and its presence in most of NOx containing streams, simultaneous removal of CO and NO using catalytic reduction seems to be an ideal strategy for the removal of these two pollutants. Noble metal and perovskite type oxides are catalysts which used for NO + CO reaction [1, 2], being noble metals more active than perovskites but also much more expensive.

Perovskite type oxides are mixed oxides with nominal formulation of ABO_3 or A_2BO_4 where A is a larger cation than B. When perovskite are used as catalysts, B usually designates a transition metal cation surrounded by six oxygen in octahedral coordination, and A is a cation of rare-earth metal coordinated by 12 oxygens [3]. Many metals are stable through the perovskite structure which provides that the A and B cations have dimension (r_A> 0.90 Å, r_B> 0.51 Å) in agreement with the limits of the so-called "tolerance factor" t (0.8 < t <1.0), defined by Goldschimdt as

$t = (r_A + r_O)/\sqrt{2}(r_B + r_O)$, and where r_A, r_B and r_O are the ionic radii for A, B and O, respectively [4]. Properties of perovskite type oxides are mainly depend on nature of A and B cations. In fact, A cations are responsible of the structure stability of perovskite, and B cation determines the catalytic activity [5]. Potentially, A and /or B cation could be replaced by other A' and B' foreign cations without destruction of matrix structure. According to the findings, such a modification leads to structural defects and oxygen excess or oxygen deficiency that are favorable for catalytic activity.

The perovskite type oxides were used in many catalytic processes including catalytic combustion or deep oxidation of volatile organic compounds (VOC's) [6-8], CO oxidation [9-11], syngas production [12, 13], among other catalytic reactions. As for other catalytic reactions, nature of catalyst plays the main role in the success of CO + NO reaction. Many researchers studied NO removal by using perovskites as catalyst. Substitution of A and B site for Fe [14-16] and Cu [17] perovskites by other transition metals, and their catalytic performance for NO reduction by CO was tested. He et al. studied the substitution of Mn by Cu and Ag in a $La_{0.8}Ce_{0.2}B_{0.4}Mn_{0.6}O_3$ (B: Cu and Ag) perovskite catalyst for CO + NO reaction and concluded that Cu is more effective than Ag [18]. The study of the use of various metals in A site, including La, Nd, Sm carried out by Ciambelli et al. [19], showed the following sequence of catalyst activity: La>Nd>Sm. The impacts and effects of the modification of the perovskite formulations by Pd were also studied [20], concluding that it is an effective element for improving the of catalytic activity of perovskites . Thus, the aim of this work is to compare the catalytic performance of perovskites with various transition metals in B site and to analyze the effect of modification of the best formulation to increase the catalytic activity. Therefore, catalysts with various formulation of $LaBO_3$ or La_2BO_4 (B: Mn, Fe, Co, Ni, Cu, Zn) were synthesized by citric acid method and tested for simultaneous removing of the NO + CO, while the most active catalyst has been selected and modified by using other transition metals in order to improve the catalytic performance. Synthesized catalysts have been characterized by using X ray diffraction (XRD), Brunauer–Emmett–Teller (BET), Temperature Programed Reduction with hydrogen (H_2-TPR), X ray Photoelectron Spectroscopy (XPS) and Scanning electron microscopy (SEM) to determine the physical-chemical properties affecting the catalytic performance.

Experimental

Catalyst preparation

The sol-gel method, as described elsewhere [6], was used to obtain the catalysts. Briefly, stoichiometric amounts of metal nitrates precursor ($La(NO_3)_3.6H_2O$, $Mn(NO_3)_2.4H_2O$, $Fe(NO_3)_3.9H_2O$, $Co(NO_3)_2.6H_2O$, $Ni(NO_3)_2.6H_2O$, $Cu(NO_3)_2.3H_2O$, $Zn(NO_3)_2.6H_2O$) were dissolved using the minimum amount of distilled water to get a clear solution (Sol). The solution was heated till 70º C on a hot plate and then an appropriate amount of the citric acid monohydrate was added (As proposed in our previous work [6], the molar ratio of citric acid to the total nitrates in the solution mixture was kept at 0.525.) The mentioned solution was stirred vigorously and heated to 80°C for dehydration and, finally, a sticky gel was obtained which was burned by heating at 200 °C on a hot plate and turned into a dark powder. The powder was calcined in two steps: at 500°C for 1 hour, and, then, at 700°C for 5 hours.

Catalyst characterization

The determination of crystalline phases was carried out using X-ray diffraction on a SIEMENS D500 diffractometer and Cu K_α radiation ($\lambda = 1.54$ Å). Diffractograms were recorded with a step of 4° per minute for 2θ between 20 and 80°. The ICSD standards were utilized as patterns for the identification of phases in the diffractograms. The particle sizes (D) were evaluated by means of the Scherrer equation ($D = K\lambda/(\beta \cos \theta)$, where K is a constant equal to 0.89, λ is the wavelength of the X-ray and β is the effective line width of the X-ray reflexion).

A Chembet-3000 apparatus was used for the H_2-TPR experiments, and that were carried out under a 10 $mL.min^{-1}$ flow of 5% H_2 in Ar, using a heating 10 °$C.min^{-1}$ up to 1000 °C.

The BET surface area (m^2/g) was analyzed and determined by N_2 adsorption at 77 K by using an F-Sorb 3400 volumetric adsorption/desorption apparatus. Prior to measurement, the samples were degassed at 150 °C under vacuum for 3 hours.

The surface composition and elemental chemical state of the samples were examined by XPS, using a Model VG ESCALAB apparatus with AlKa X-ray source. The binding energies were calibrated with respect to the signal for adventitious carbon (binding energy = 284.6 eV).

Finally, the surface morphology was determined by SEM using a Hitachi S3000N electron microscope (JEOL, Japan).

Catalytic studies

Figure 1 shows a simple scheme of catalytic set-up used. The CO + NO reaction was carried out in a straight quartz reactor (l = 2 cm, i.d. = 0.8 cm, where the 200 mg catalyst was inserted between two quartz wool plugs) at different temperatures under atmospheric pressure. Before reaction tests, the catalysts should be pretreated with air (40 cm^3min^{-1}) at 300°C for 2 hours. The total flow rate was 200 cm^3min^{-1} and the gas composition was 3000 ppm NO and 3000 ppm CO balanced with Ar. Gas hourly space velocity (GHSV) was fixed about 12000 h^{-1} and the reaction temperature was controlled by using K-type thermocouple.

A Shimadzu 2010 gas chromatograph (GC), equipped with a TCD detector and a HP-Molesieve (Agilent, USA) column (l = 30 m, i.d. = 0.53 mm) with helium as carrier gas, was used to analyze the feed and product gases.

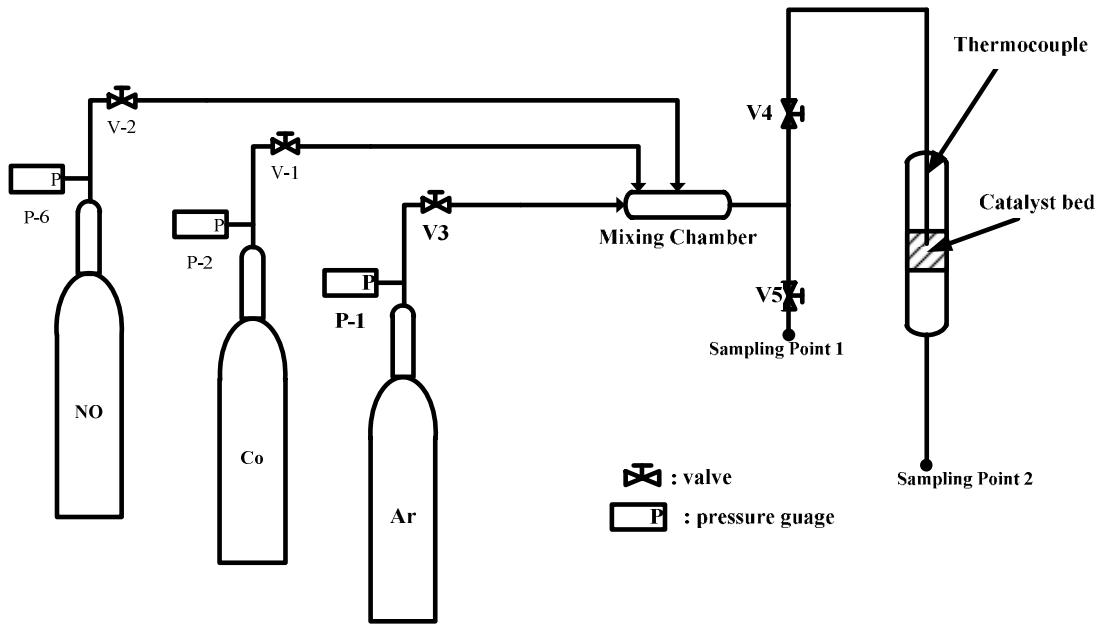

Figure 1: Simple scheme of catalytic test set up for CO+NO reaction.

Results

Catalysts characterization

The XRD results of $LaBO_3$ (B: Mn, Fe, Co, Ni) and La_2CuO_4 catalysts were presented in Figure 2 and, as it is possible to be seen, the XRD pattern of $LaMnO_3$, $LaFeO_3$, $LaCoO_3$, $LaNiO_3$ and La_2CuO_4 catalysts are in agreement with standard patterns ICSD 082315, ICSD 084941, ICSD 201763, ICSD 067717 and ICSD 019003, respectively. La_2CuO_4 XRD pattern shows the presence of some CuO (at 2Θ about 39 and 35).

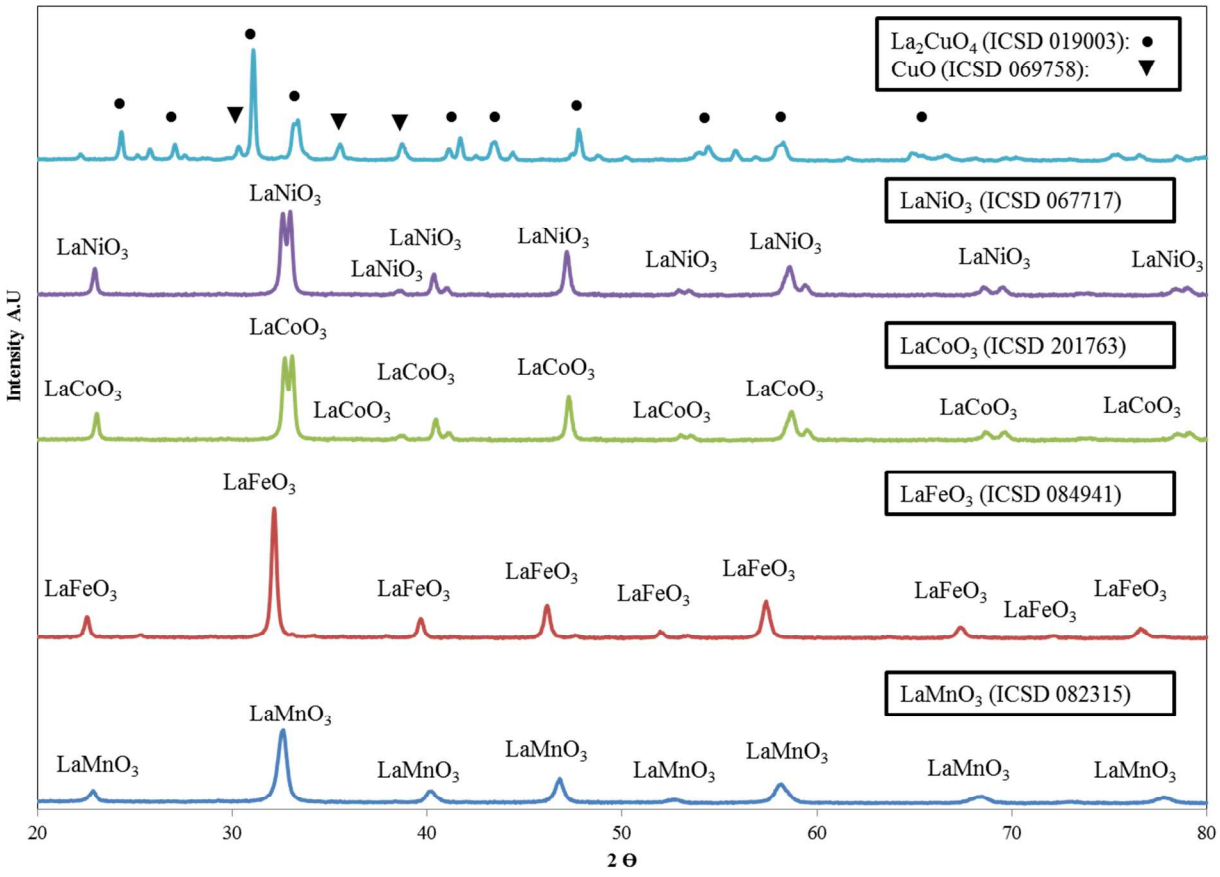

Figure 2: XRD results of $LaBO_3$ B (Mn, Fe, Co, Ni) and La_2CuO_4 catalysts

The Figure 3 shows XRD patterns of modified $LaFeO_3$ catalysts compared with that of the pure $LaFeO_3$ to feature the effect of the incorporation of the modifier metals in the structure of

$LaFeO_3$. Thus, the structure of $LaFe_{0.7}M_{0.3}O_3$ (M: Mn, Co and Cu) is similar to $LaFeO_3$ itself and, consequently, it can be concluded that there is not any second metal oxide phase in the catalyst structure. Figure 3b, where a comparison of the catalysts main peak is shown, reveals a shift due to the metals insertion in the $LaFeO_3$ structure. The change of the unit cell size shown in table 1 proves that the metals were inserted into the $LaFeO_3$ crystalline structure and did not form a second crystalline phase.

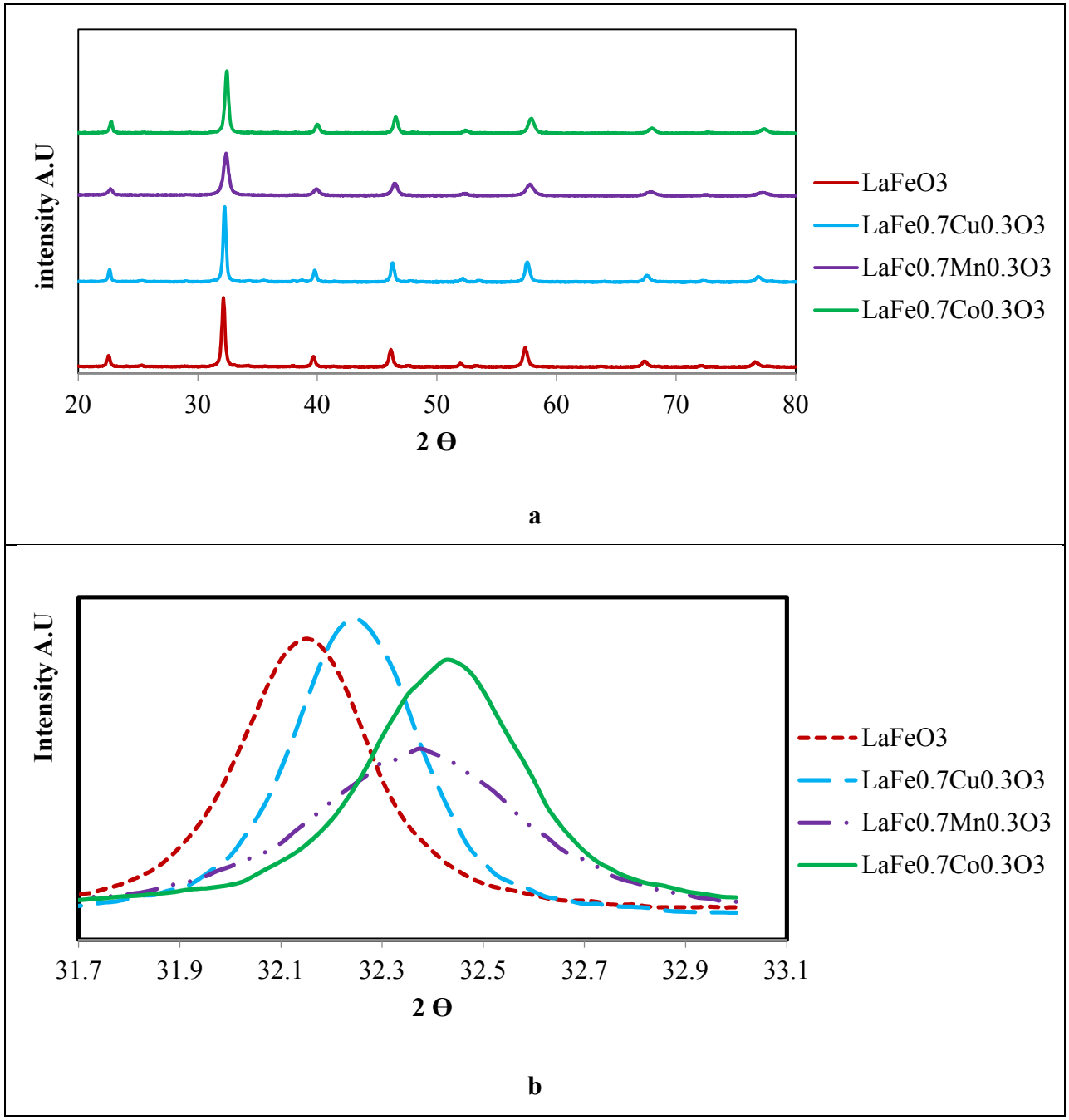

Figure 3: XRD patterns of modified $LaFeO_3$ catalysts compared with pure $LaFeO_3$ (a) and 2Θ shift for different metals as modifier (b)

Table 1: Unit cell parameters and cell volume for $LaFeO_3$ catalyst before and after modification by other transition metals.

Catalyst	a (Å)	b (Å)	c (Å)	Volume
$LaFeO_3$	5.56	5.56	7.89	243.90
$LaFe_{0.7}Cu_{0.3}O_3$	5.54	5.54	7.86	241.66
$LaFe_{0.7}Mn_{0.3}O_3$	5.52	5.53	7.83	238.92
$LaFe_{0.7}Co_{0.3}O_3$	5.51	5.52	7.81	237.81

XPS studies

The surface composition of $LaFeO_3$, $LaMnO_3$ and $LaFe_{0.7}Mn_{0.3}O_3$ catalysts was determined. In Figure 4, XPS spectra of $2p_{3/2}$ area for Fe in $LaFeO_3$ (a), Mn in $LaMnO_3$ (b), Fe in $LaFe_{0.7}Mn_{0.3}O_3$ (c) and Mn in $LaFe_{0.7}Mn_{0.3}O_3$ can be seen. In Figure 4, peaks on about 710 ev, 713 ev, 641 ev and 644 ev are assigned to Fe(III), Fe(IV), Mn(III) and Mn(IV), respectively.

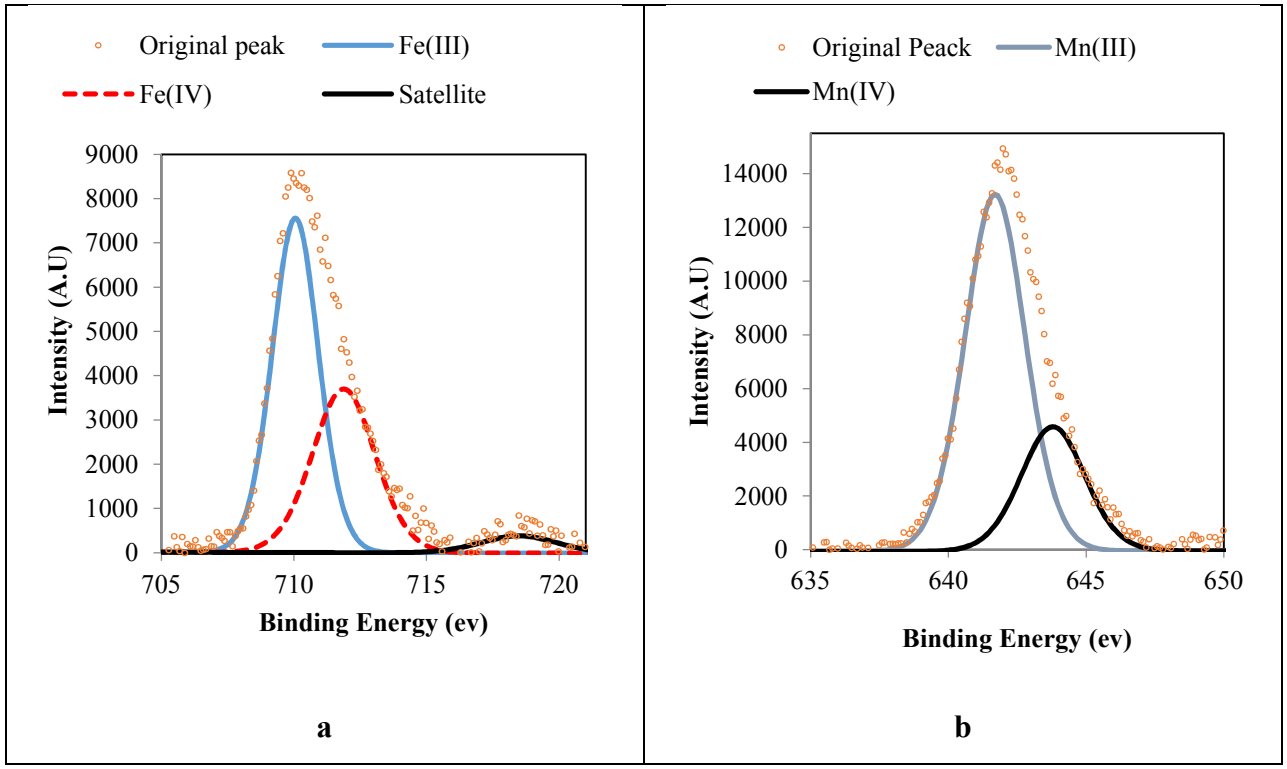

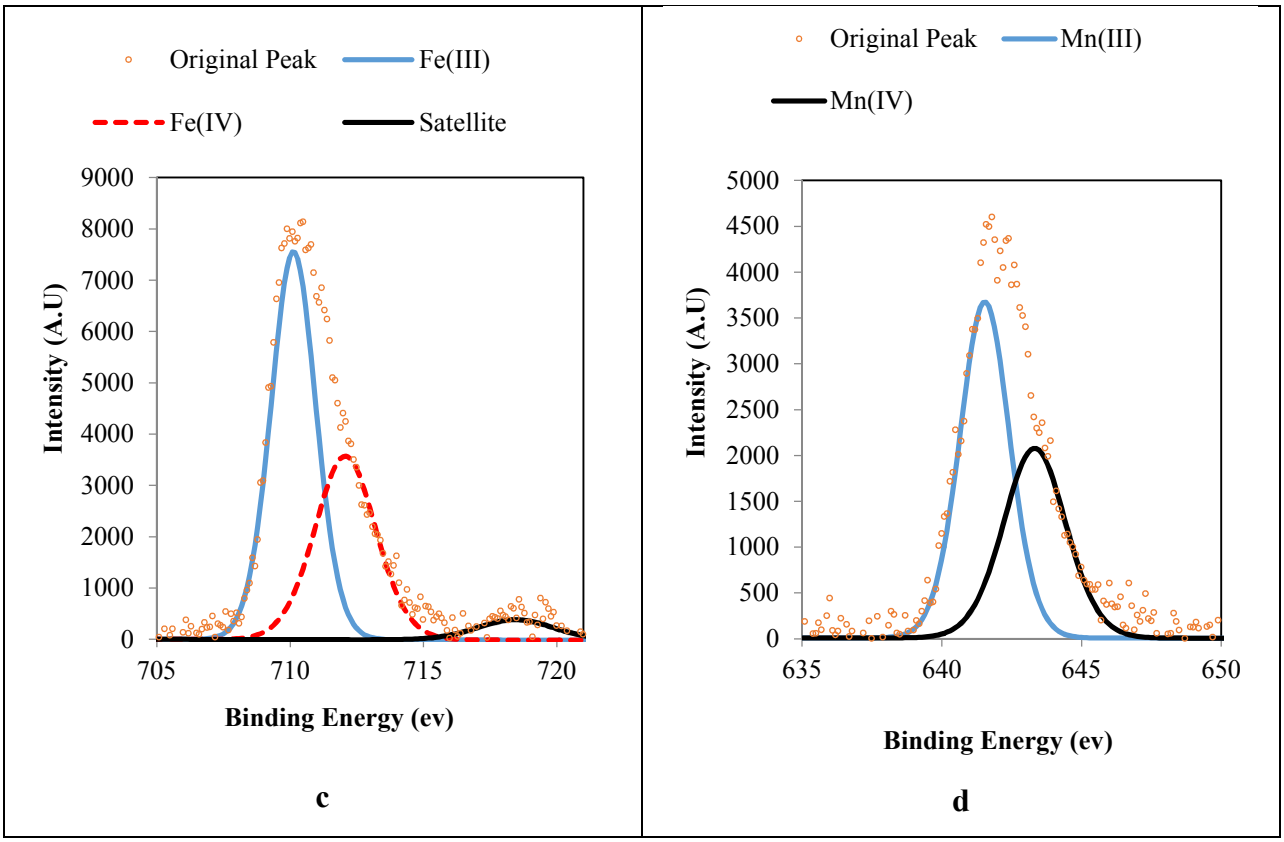

Figure 4: XPS spectra of $2p_{3/2}$ area for Fe in $LaFeO_3$ (a), Mn in $LaMnO_3$ (b), Fe in $LaFe_{0.7}Mn_{0.3}O_3$ (c) and Mn in $LaFe_{0.7}Mn_{0.3}O_3$.

In Figure 5, the XPS spectra of 1s area for oxygen in $LaFeO_3$, $LaMnO_3$ and $LaFe_{0.7}Mn_{0.3}O_3$ are presented. In the three spectra, the first peak around the 529 ev corresponds to lattice oxygen, the second peak around the 531.5 ev is assigned to surface oxygen and the third peak at about 533.5 ev belongs to adsorbed water.

a

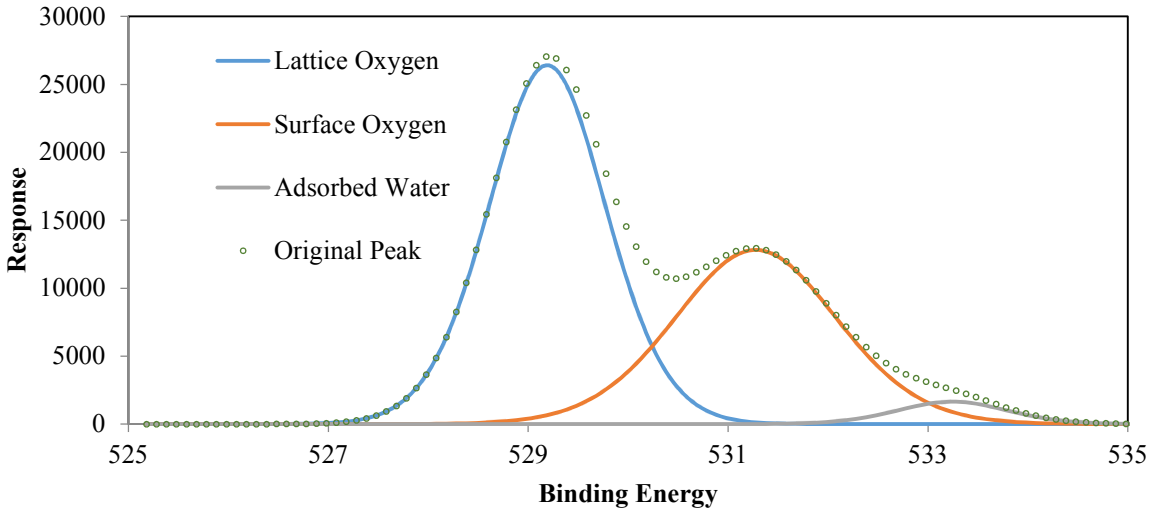
30000
25000
20000
15000
10000
5000
0
Response
Lattice Oxygen
Surface Oxygen
Adsorbed Water
Original Peak
525
527
529
531
533
535
Binding Energy

b

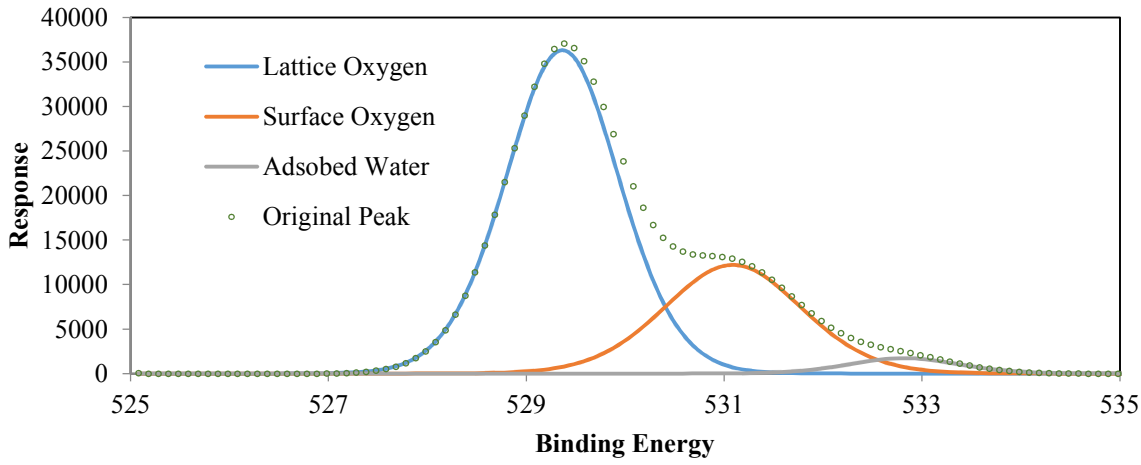
40000
35000
30000
25000
20000
15000
10000
5000
0
Response
Lattice Oxygen
Surface Oxygen
Adsobed Water
Original Peak
525
527
529
531
533
535
Binding Energy

c

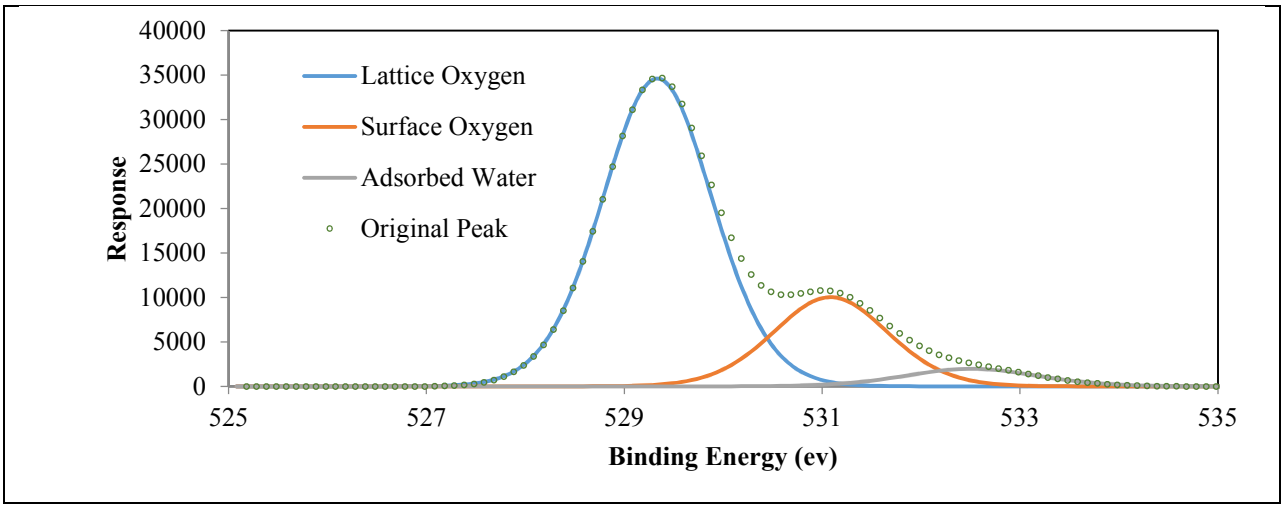

Figure 5: XPS spectra of O 1s area for oxygen in $LaFeO_3$, $LaMnO_3$ and $LaFe_{0.7}Mn_{0.3}O_3$

BET results

Surface area of catalysts were shown in table 2. $LaMnO_3$ shows the highest surface area and $LaFe_{0.7}Mn_{0.3}O_3$ the lowest one. The $LaFe_{0.7}Mn_{0.3}O_3$ presents a surface area in between the two raw peovskite.

Table 2: Surface area of $LaFeO_3$, $LaMnO_3$ and $LaFe_{0.7}Mn_{0.3}O_3$

Catalyst Number	**Catalyst Formulation**	**BET (m^2/gr)**
1	$LaFeO_3$	7.8
2	$LaMnO_3$	40.5
3	$LaCoO_3$	25.7
4	$LaFe_{0.7}Co_{0.3}O_3$	18.9
5	$LaFe_{0.7}Cu_{0.3}O_3$	17.71
6	$LaFe_{0.7}Mn_{0.3}O_3$	32.3

SEM analysis

Figure 6 presents the SEM images of the catalysts where a defined morphology is not observed.

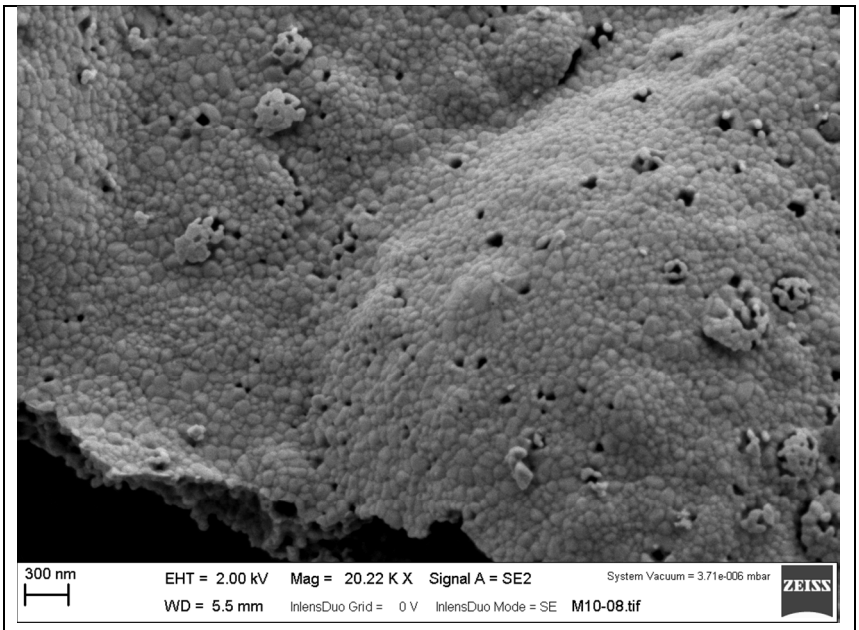
300 nm
EHT = 2.00 kV
Mag = 20.22 K X
Signal A = SE2
System Vacuum = 3.71e-006 mbar
WD = 5.5 mm
InlensDuo Grid = 0 V
InlensDuo Mode = SE
M10-08.tif
ZEISS

a

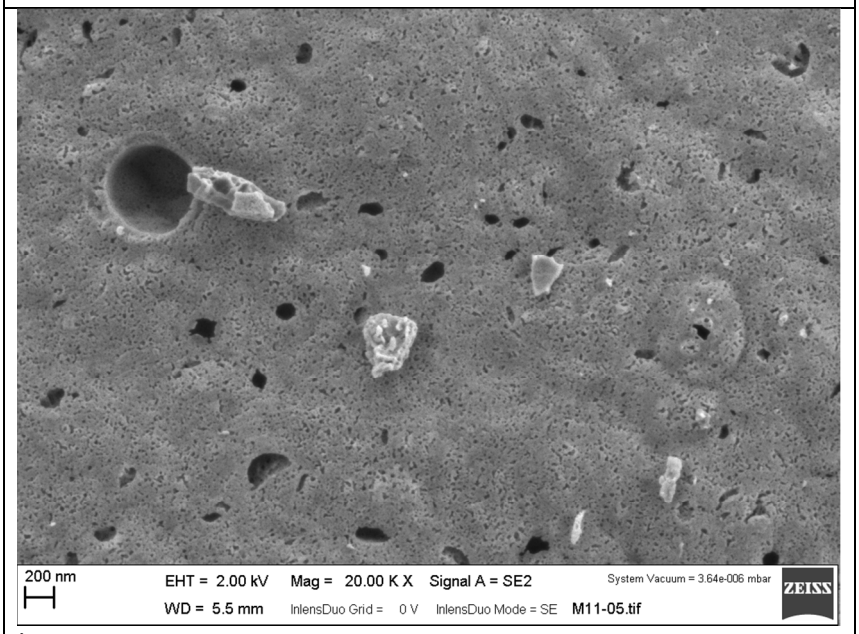
200 nm
EHT = 2.00 kV
Mag = 20.00 K X
Signal A = SE2
System Vacuum = 3.64e-006 mbar
WD = 5.5 mm
InlensDuo Grid = 0 V
InlensDuo Mode = SE
M11-05.tif
ZEISS

b

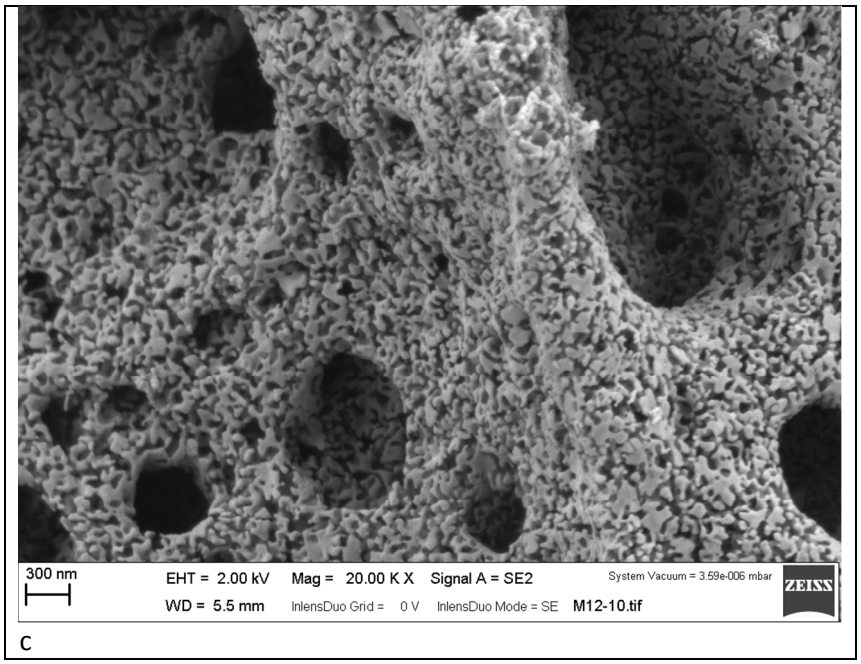

Figure 6: SEM graph of a: $LaFeO_3$, b: $LaFe_{0.7}Mn_{0.3}O_3$ and c: $LaMnO_3$

H_2- TPR results

The reducible active sites of each catalyst were analyzed by using H_2- TPR method, and the results are shown in Figure 7. The TPR profile for $LaFeO_3$ shows two significant peaks starting from 410°C which can be assigned to the reduction of Fe(IV) and Fe(III), respectively [21]. In addition, two significant peaks were revealed for $LaMnO_3$ related to the reduction of Mn(IV) and Mn(III) starting from about 200°C and 700°C [22, 23].

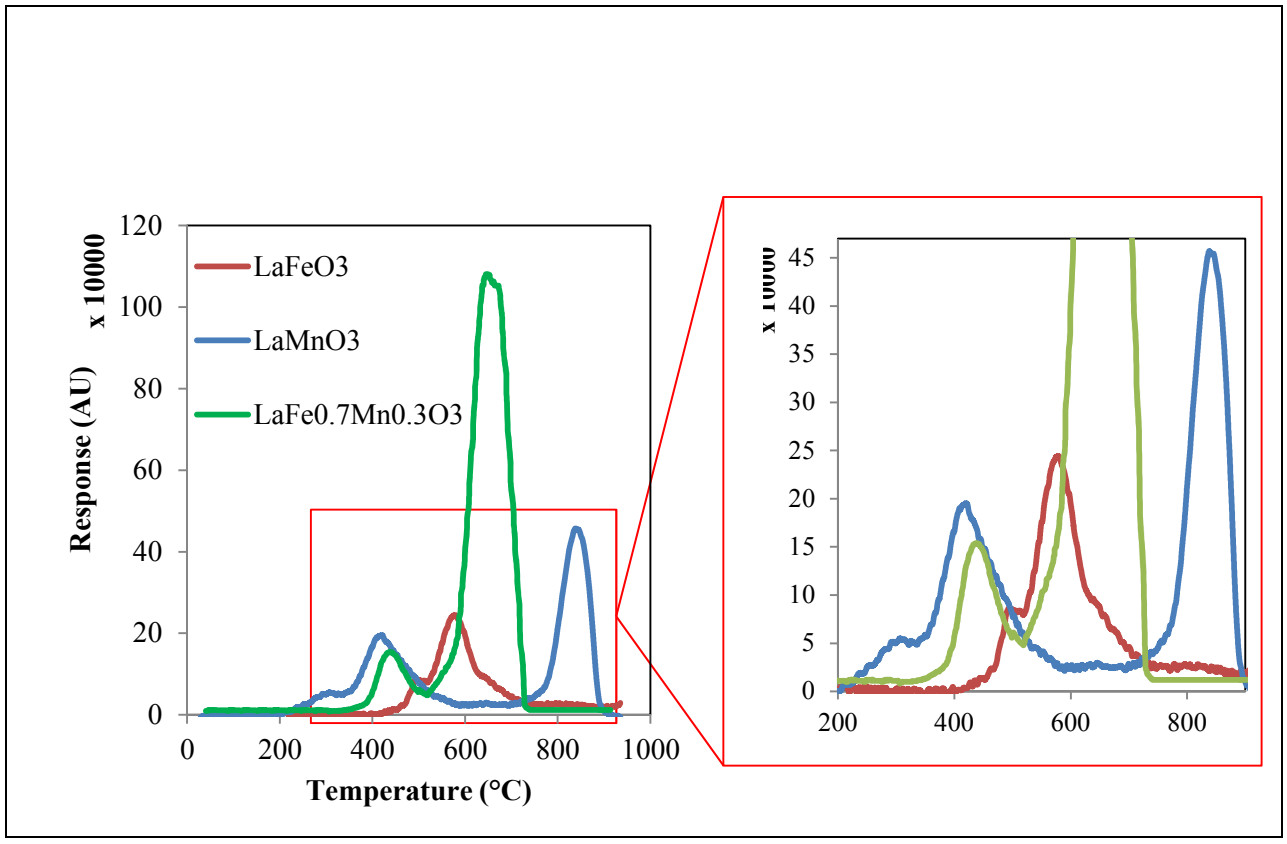

Figure 7: TPR results for $LaFeO_3$, $LaMnO_3$ and $LaFe_{0.7}Mn_{0.3}O_3$.

For $LaFe_{0.7}Mn_{0.3}O_3$, the H_2-TPR profile change significantly and two significant peaks were observed; first peak starting from about 330°C can be assigned to the reduction of Mn(IV) and the second peak was a possible mixture of peaks related to the reduction of Fe(IV), Fe(III) and Mn(III). Additionally, it is clear from Figure 7 that the amount of reducible active sites for $LaFe_{0.7}Mn_{0.3}O_3$ was significantly increased respect to $LaFeO_3$ catalyst.

Catalytic activity for CO + NO removal

The catalytic performance of catalysts is shown in Figure 8, where it is observed that, as expected [3, 24], the NO and CO conversion increased with the reaction temperature for all catalysts. The difference between catalytic activities increased with the reaction temperature, being the largest at 400°C. At this temperature, the sequence of activity was $LaFeO_3$> $LaCoO_3$> La_2CuO_4> $LaNiO_3$> $LaMnO_3$> $LaZnO_3$, so, $LaFeO_3$ is the most active catalyst.

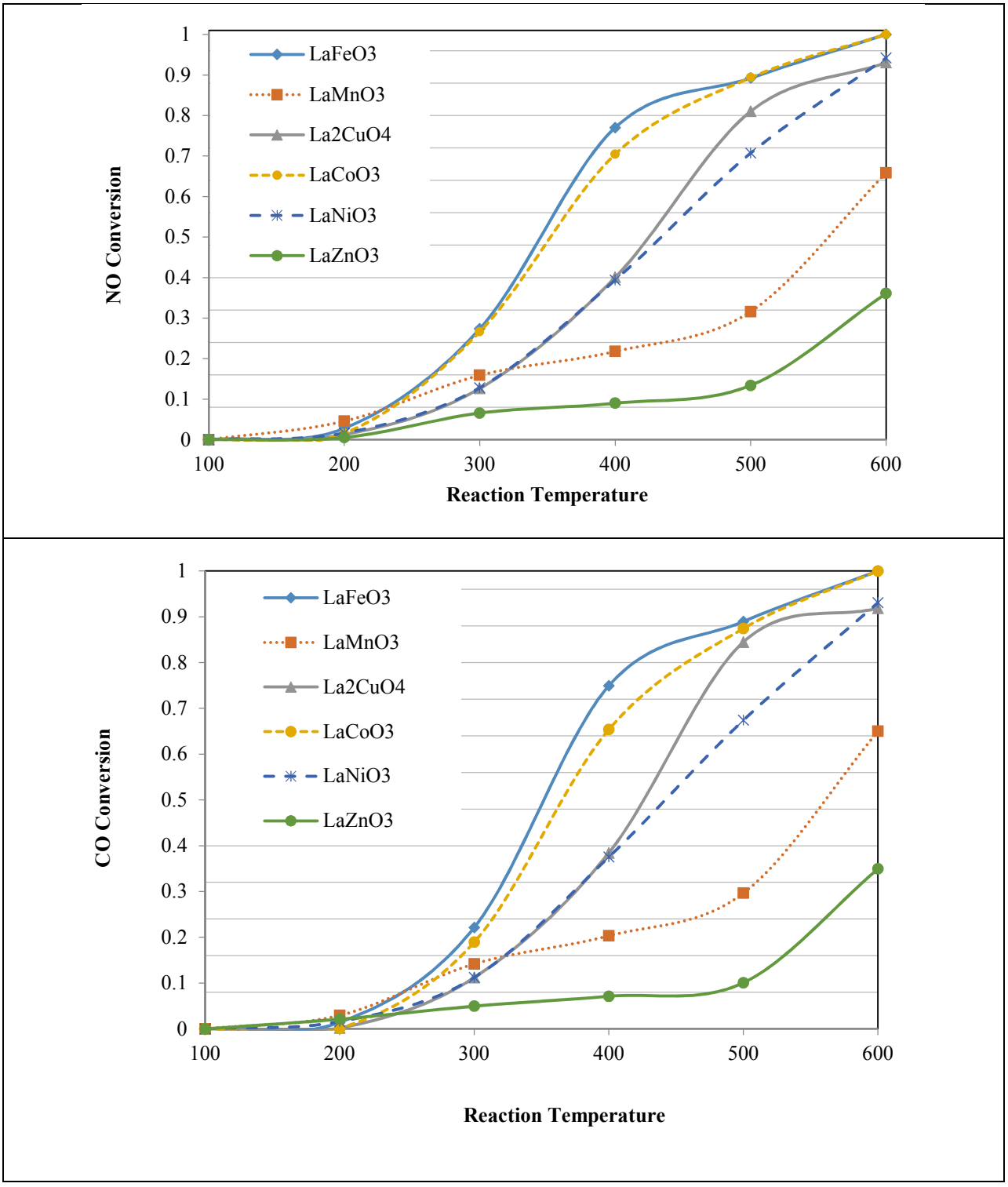

Figure 8: Catalytic activity of $LaBO_3$ (B: Mn, Fe, Co, Ni and Zn) and La_2CuO_4 for NO reduction by CO.

For CO + NO reaction, the N_2 is the desired product being N_2O an intermediate and undesired product due its greenhouse effect (10 times larger than that of the CO). In Figure 9, N_2O and N_2 yield of catalysts versus reaction temperature is shown.

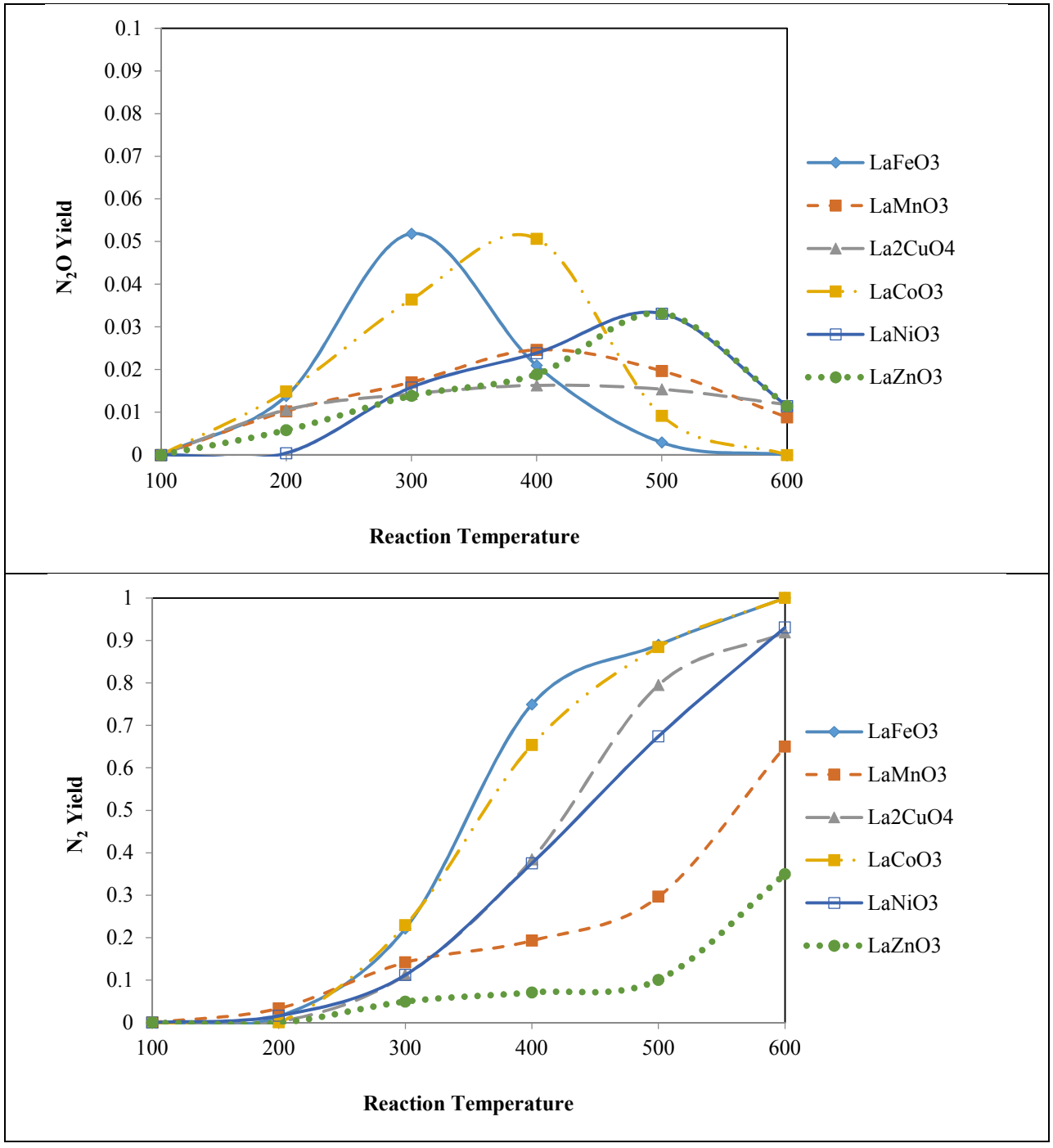

Figure 9: N_2O and N_2 of yield $LaBO_3$ (B: Mn, Fe, Co, Ni and Zn) and La_2CuO_4 catalysts.

The N_2O yield shows a volcano type behavior and the maximum in the N_2O yield is reached for each catalyst at different reaction temperatures. The yield of N_2O is higher for the more active catalysts including $LaFeO_3$ and $LaCoO_3$ because of the higher NO conversion. The maximum N_2O yield is about 5% at 300ºC for the most active catalyst ($LaFeO_3$) and decreased by increasing reaction temperature reaching zero at 500ºC approximately. Based on results of Figure 8 and 9, the $LaFeO_3$ is the most active catalyst with 100% N_2 yield at high reaction temperatures and, therefore, this formulation has been selected to be modified ($LaFe_{0.7}M_{0.3}O_3$, being M: Mn, Co and Cu) using other active transition metals [6-8].

In Figure 10, the NO, CO conversion, N_2O yield and N_2 yield for the $LaFe_{0.7}M_{0.3}O_3$ catalyst is shown. It is observed that the addition of Mn increased catalyst activity significantly, while addition of Cu and Co has not a significant effect at low temperatures and even resulted in a decrease of the activity at high reaction temperatures. Besides, from Figure 10.b it is deduced that addition of Mn, increases the N_2O selectivity at low temperature, however, the N_2O selectivity is acceptable and reaches zero at high temperatures.

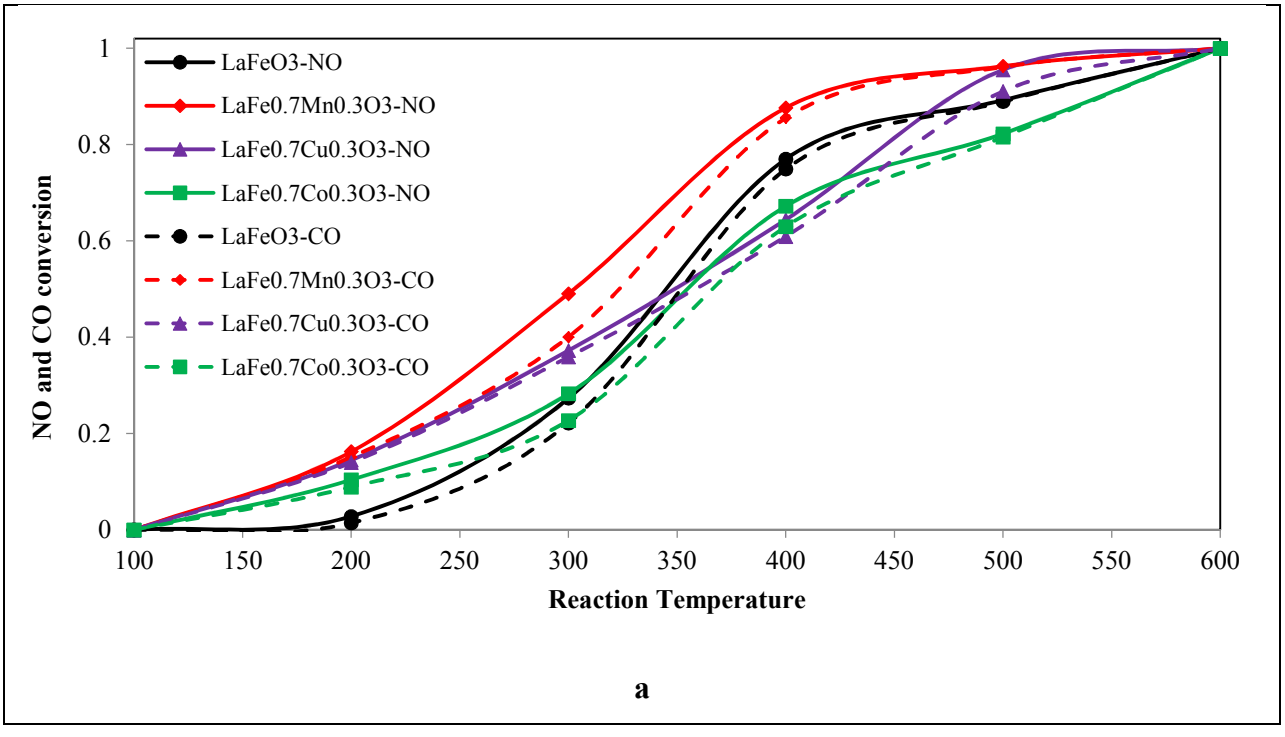

a

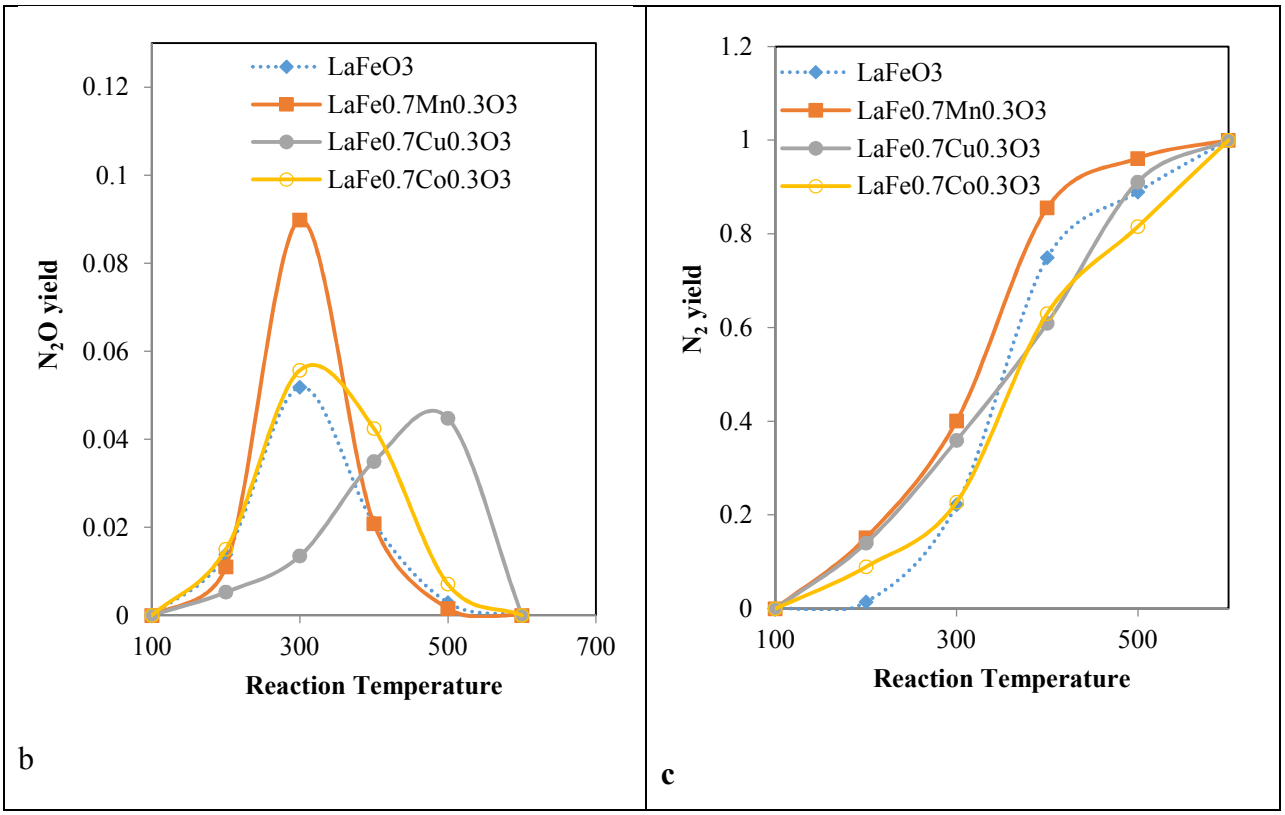

Figure 10: NO conversion (a) and N_2O yield (b) for $LaFe_{0.7}M_{0.3}O_3$ (M: Mn, Cu and Co) catalysts.

Discussion

The modification of $LaFeO_3$ by Mn resulted in an enhancement in catalytic activity for NO + CO reaction. Based on results which were presented in Figure 3, The $LaFe_{0.7}Mn_{0.3}O_3$ catalyst has the similar crystal structure to $LaFeO_3$ which means that the modifier metal (Mn) were not incorporated in any other metal oxide phase except the $LaFe_{0.7}Mn_{0.3}O_3$. Also, slight shifts on XRD peaks of $LaFe_{0.7}Mn_{0.3}O_3$ in comparison to $LaFeO_3$, is a result of unit cell size change (table 2) which happened because of Mn insertion into the $LaFeO_3$ crystal structure. From Figure 4 and based on XPS analysis, it is deduced that the surface amount of Mn(IV) was increased for $LaFe_{0.7}Mn_{0.3}O_3$ respect to $LaMnO_3$, this is because after incorporation of Mn in $LaFeO_3$ structure, the ratio of Mn(IV) to Mn(III) increased from 0.373 to 0.694 for $LaFe_{0.7}Mn_{0.3}O_3$. In fact, the simultaneous use of Mn with other transition metals as B ion leads to an increase in Mn(IV) to Mn(III) ratio [3]. From the stoichiometric point of view, the Mn should be in Mn(III) state to achieve the neutral compound. As consequence of the change from Mn (III) to Mn (IV),

structural defects should be created to maintain the compound neutrality. Thus, the structural defects can be seen as an increase of surface oxygen vacancies as a result of the high Mn(IV) concentration in composition. On the other hand, the ratio of Fe(IV) to Fe(III) is 0.665 and 0.644 for LaFeO3 and $LaFe_{0.7}Mn_{0.3}O_3$, respectively, so, it is almost constant. In addition, based on the peaks area on Figure 5, the surface oxygen to lattice oxygen ratio is 0.301, 0.673 and 0.408 for $LaFe_{0.7}Mn_{0.3}O_3$, $LaFeO_3$ and $LaMnO_3$, respectively. Thus, the lower surface oxygen to lattice oxygen ratio of $LaFe_{0.7}Mn_{0.3}O_3$ confirms the larger amount of vacancies structural defects created. According to the mechanism established for CO + NO reaction [20, 24] by increasing the vacancies, the surface adsorption of the NO and CO reactants was facilitated and, as a result, the catalytic activity was improved [24, 25]. Besides, it is clear from H_2-TPR results (Figure 7) that the amount of reducible active sites for $LaFe_{0.7}Mn_{0.3}O_3$ catalyst was significantly increased respect to $LaFeO_3$ catalyst. This is because the area of reduction peak about 600°C of $LaFe_{0.7}Mn_{0.3}O_3$ is significantly larger respect to the same peak for $LaFeO_3$. Since NO + CO is an oxidation/reduction reaction; the number of reducible active sites plays an important role. Thus, H_2-TPR results are also in agreement with XPS analysis.

On the other hand, the $LaFe_{0.7}Mn_{0.3}O_3$ presents a surface area in between the two raw peovskites. This indicates that surface area cannot be the determining parameter for activity of synthesized catalysts. Also, there is not any significant change in the surface area of the synthesized catalysts before and after the modification. Moreover, SEM results are also in agreement with BET results as any specific surface morphology was not observed for synthesized catalysts.

Therefore, the enhancement in Mn(IV) to Mn(III) ratio, an increase in amount of surface vacancies and on the reducible sites, are the key parameters determining the catalytic activity.

Conclusion

In the present study, different perovskite formulations, including La and a series of transition metals Mn, Fe, Co, Ni, Cu and Zn, were synthesized by using citrate method and tested in CO+NO reaction. $LaFeO_3$ was selected for modification by using Mn, Co and Cu because its superior activity in comparison to other formulations. The catalytic activity of $LaFeO_3$ which was modified by Mn ($LaFe_{0.7}M_{0.3}O_3$) was increased significantly. The XRD analysis proved the

perovskite structure for catalysts and the insertion of modifier metals into the crystal structure of $LaFeO_3$. The XPS analysis revealed that the increase of Mn (IV) to Mn (III) ratio, resulting in the enhancement of the structural defects. The mentioned defects increased the reducible active sites of $LaFe_{0.7}M_{0.3}O_3$ catalyst and, as a consequence, the catalytic activity for NO+CO reaction, which is a oxidation/reduction reaction, is improved.

Acknowledgement

Financial supports from the Iran National Science Foundation (INSF) are gratefully acknowledged.

References

(1) Belessi, V.; Trikalitis, P.; Ladavos, A.; Bakas, T.; Pomonis, P. Structure and Catalytic Activity of $La_{1-x}FeO_3$ System (x=0.00, 0.05, 0.10, 0.15, 0.20, 0.25, 0.35) for the NO+CO Reaction. *App. Catal. A: Gen*. **1999**, *177* (1), 53.

(2) Zhu, J.; Thomas, A. Perovskite-type Mixed Oxides as Catalytic Material for NO Removal. *App. Catal. B: Environ*. **2009**, *92*, 225.

(3) Zhang, R.; Villanueva, A.; Alamdari, H.; Kaliaguine, S. Reduction of NO by CO over Nanoscale $LaCo_{1-x}Cu_xO_3$ and $LaMn_{1-x}Cu_xO_3$ Perovskites. *J. Mol. Catal. A: Chem*. **2006**, *258*, 22.

(4) Femina, P.; Sanjay, P. $LaCoO_3$ Perovskite Catalysts for the Environmental Application of Auto Motive CO Oxidation. *Res. j. recent sci*. **2012**, *1*, 178.

(5) Gallagher, P.; Johnson, D.; Vogel, E. Preparation, Structure, and Selected Catalytic Properties of the System $LaMn_{1-x}Cu_xO_{3-y}$. *J. Am. Ceram. Soc.* **1977**, *60*, 28.

(6) Oskoui, S. A.; Niaei, A.; Tseng, H.-H.; Salari, D.; Izadkhah, B.; Hosseini, S.A. Modeling Preparation Condition and Composition–Activity Relationship of Perovskite-Type $La_xSr_{1-x}Fe_yCo_{1-y}O_3$ Nano Catalyst. *ACS. Comb. Sci*. **2013**, *15*, 609.

(7) Hosseini, S. A.; Salari, D.; Niaei, A.; Oskoui, S. A. Physical–Chemical Property and Activity Evaluation of $LaB_{0.5}Co_{0.5}O_3$ (B= Cr, Mn, Cu) and $LaMn_xCo_{1-x}O_3$ (x= 0.1, 0.25, 0.5) Nano Perovskites in VOC Combustion. *J. Ind. Eng. Chem*. **2013**, *19*, 1903.

(8) Hosseini, S. A.; Sadeghi, M. T.; Alemi, A.; Niaei, A.; Salari, D.; Kafi-Ahmadi, L. Synthesis, Characterization, and Performance of $LaZn_xFe_{1-x}O_3$ Perovskite Nanocatalysts for Toluene Combustion. *Chinese J. Catal*. **2010**, *31*, 747.

(9) Cimino, S.; Colonna, S.; De Rossi, S.; Faticanti, M.; Lisi, L.; Pettiti, I.; Porta, P. Methane Combustion and CO Oxidation on Zirconia-Supported La, Mn Oxides and $LaMnO_3$ Perovskite. *J. Catal*. **2002**, *205*, 309.

(10) Zhang-Steenwinkel, Y.; Beckers, J.; Bliek, A. Surface Properties and Catalytic Performance in CO Oxidation of Cerium Substituted Lanthanum–Manganese Oxides. *App. Catal. A: Gen*. **2002**, *235*, 79.

(11) Tascon, J.; Tejuca, L. G. Catalytic Activity of Perovskite-type Oxides $LaMeO_3$. *React. Kinet. Catal. Lett*. **1980**, *15*, 185.

(12) Choudhary, V.; Uphade, B.; Belhekar, A. Oxidative Conversion of Methane to Syngas over $LaNiO_3$ Perovskite with or without Simultaneous Steam and CO_2 Reforming Reactions: Influence of Partial Substitution of La and Ni. *J. Catal*. **1996**, *163*, 312.

(13) Wang, H.; Cong, Y.; Yang, W. Investigation on the Partial Oxidation of Methane to Syngas in a Tubular $Ba_{0.5}Sr_{0.5}Co_{0.8}Fe_{0.2}O_{3-\delta}$ Membrane Reactor. *Catal. Today*. **2003**, *82*, 157.

(14) Giannakas, A.; Ladavos, A.; Pomonis, P. Preparation, Characterization and Investigation of Catalytic Activity for NO+CO Reaction of $LaMnO_3$ and $LaFeO_3$ Perovskites Prepared via Microemulsion Method. *App. Catal. B: Environ*. **2004**, *49*, 147.

(15) Giannakas, A.; Leontiou, A.; Ladavos, A.; Pomonis, P. Characterization and Catalytic Investigation of NO+CO Reaction on Perovskites of the General Formula $La_xM_{1-x}FeO_3$ (M= Sr and/or Ce) Prepared via a Reverse Micelles Microemulsion Route. *App. Catal. A: Gen*. **2006**, *309*, 254.

(16) Belessi, V.; Costa, C.; Bakas, T.; Anastasiadou, T.; Pomonis, P.; Efstathiou, A. Catalytic Behavior of La–Sr–Ce–Fe–O Mixed Oxidic/Perovskitic Systems for the NO+ CO and NO+ CH_4+O_2 (Lean-NO x) Reactions. *Catal. Today*. **2000**, *59*, 347.

(17) Zhang, R.; Villanueva, A.; Alamdari, H.; Kaliaguine, S. Catalytic Reduction of NO by Propene over $LaCo_{1-x}Cu_xO_3$ Perovskites Synthesized by Reactive Grinding. *App. Catal. B: Environ*. **2006**, *64*, 220.

(18) He, H.; Liu, M.; Dai, H.; Qiu, W.; Zi, X. An Investigation of NO/CO Reaction over Perovskite-type Oxide $La_{0.8}Ce_{0.2}B_{0.4}Mn_{0.6}O_3$ (B= Cu or Ag) Catalysts Synthesized by Reverse Microemulsion. *Catal. Today*. **2007**, *126*, 290.

(19) Ciambelli, P.; Cimino, S.; De Rossi, S.; Lisi, L.; Minelli, G.; Porta, P.; Russo, G. $AFeO_3$(A= La, Nd, Sm) and $LaFe_{1-x}Mg_xO_3$ Perovskites as Methane Combustion and CO Oxidation Catalysts: Structural, Redox and Catalytic Properties. *App. Catal. B: Environ*. **2010**, *29*, 239.

(20) Ziaei-Azad, H.; Khodadadi, A.; Esmaeilnejad-Ahranjani, P.; Mortazavi, Y. Effects of Pd on Enhancement of Oxidation Activity of $LaBO_3$ (B= Mn, Fe, Co and Ni) Pervoskite Catalysts for Pollution Abatement from Natural Gas Fueled Vehicles. *App. Catal. B: Environ*. **2011**, *102*, 62.

(21) Li, R.; Yu, C.; Shen, S. Partial Oxidation of Methane to Syngas Using Lattice Oxygen of $La_{1-x}Sr_xFeO_3$ Perovskite Oxide Catalysts Instead of Molecular Oxygen. *J. Energy Chem*. **2002**, *11*, 137.

(22) Magalhães, F.; Moura, F. C. C.; Ardisson, J. D.; Lago, R. M. $LaMn_{1-x}Fe_xO_3$ and $LaMn_{0.1-x}Fe_{0.90}Mo_xO_3$ Perovskites: Synthesis, Characterization and Catalytic Activity in H_2O_2 Reactions. *Mat. Res*. **2008**, *11*, 307.

(23) Fang, H.; Kun, Z.; Huang, Z.; Guoqiang, W.; Haibin, L. Synthesis of Three-Dinmentionally Ordered Macroporous $LaFeO_3$ Perovskites and Their Performance for Chemical-Looping Reforming of Methane. *Chinese J. Catal*. **2013**, *34*, 1242.

(24) Leontiou, A.; Ladavos, A.; Pomonis, P. Catalytic NO Reduction with CO on $La_{1-x}Sr_x(Fe^{3+}/Fe^{4+})O_{3\pm\delta}$ Perovskite-type Mixed Oxides (x = 0.00, 0.15, 0.30, 0.40, 0.60, 0.70, 0.80, and 0.90). *App. Catal. A: Gen*. **2013**, *241*, 133.

(25) Misono, M. Recent Progress in the Practical Applications of Heteropolyacid and Perovskite Catalysts: Catalytic Technology for the Sustainable Society. *Catal. Today*. **2009**, *144*, 285.

List of Figure captions

Figure 1: Simple scheme of catalytic test set up for CO+NO reaction.

Figure 2: XRD results of $LaBO_3$ B (Mn, Fe, Co, Ni) and La_2CuO_4 catalysts

Figure 3: XRD patterns of modified $LaFeO_3$ catalysts compared with pure $LaFeO_3$ (a) and 2Θ shift for different metals as modifier (b)

Figure 4: XPS spectra of $2p_{3/2}$ area for Fe in $LaFeO_3$ (a), Mn in $LaMnO_3$ (b), Fe in $LaFe_{0.7}Mn_{0.3}O_3$ (c) and Mn in $LaFe_{0.7}Mn_{0.3}O_3$.

Figure 5: XPS spectra of O 1s area for oxygen in $LaFeO_3$, $LaMnO_3$ and $LaFe_{0.7}Mn_{0.3}O_3$

Figure 6: SEM graph of a: $LaFeO_3$, b: $LaFe_{0.7}Mn_{0.3}O_3$ and c: $LaMnO_3$

Figure 7: TPR results for $LaFeO_3$, $LaMnO_3$ and $LaFe_{0.7}Mn_{0.3}O_3$.

Figure 8: Catalytic activity of $LaBO_3$ (B: Mn, Fe, Co, Ni and Zn) and La_2CuO_4 for NO reduction by CO.

Figure 9: N_2O and N_2 of yield $LaBO_3$ (B: Mn, Fe, Co, Ni and Zn) and La_2CuO_4 catalysts.

Figure 10: NO conversion (a) and N_2O yield (b) for $LaFe_{0.7}M_{0.3}O_3$ (M: Mn, Cu and Co) catalysts.

For Table of Contents Only